






Article

Green Emissive Copper(I) Coordination Polymer Supported by the Diethylpyridylphosphine Ligand as a Luminescent Sensor for Overheating Processes

Kamila R. Enikeeva ¹, Aliia V. Shamsieva ¹, Anna G. Strelnik ¹, Robert R. Fayzullin ¹, Dmitry V. Zakharychev ¹, Ilya E. Kolesnikov ², Irina R. Dayanova ¹, Tatiana P. Gerasimova ¹, Igor D. Strelnik ^{1,*}, Elvira I. Musina ¹, Andrey A. Karasik ¹ and Oleg G. Sinyashin ¹

¹ Arbuzov Institute of Organic and Physical Chemistry, FRC Kazan Scientific Center, Russian Academy of Sciences, 8 Arbuzov Street, 420088 Kazan, Russia

² Centre for Optical and Laser Materials Research, Research Park of Saint Petersburg State University, 5 Ulianovskaya Street, 198504 Saint Petersburg, Russia

* Correspondence: igorstrelnik@iopc.ru

Abstract: Tertiary diethylpyridylphosphine was synthesized by the reaction of pyridylphosphine with bromoethane in a subbasic medium. The reaction of phosphine with the copper(I) iodide led to the formation of a copper(I) coordination polymer, which, according to the X-ray diffraction data, has an intermediate structure with a copper-halide core between the octahedral and stairstep geometries of the Cu₄I₄ clusters. The obtained coordination polymer exhibits a green emission in the solid state, which is caused by the ³(M+X)LCT transitions. The heating up of the copper(I) coordination polymer to 138.5 °C results in its monomerization and the formation of a new solid-state phase. The new phase exhibits a red emission, with the emission band maximum at 725 nm. According to the experimental data and quantum chemical computations, it was concluded that depolymerization probably leads to a complex that is formed with the octahedral structure of the copper-halide core. The resulting solid-state phase can be backward-converted to the polymer phase via recrystallization from the acetone or DMF. Therefore, the obtained coordination polymer can be considered a sensor or detector for the overheating of processes that should be maintained at temperatures below 138 °C (e.g., engines, boiling liquids, solar heat systems, etc.).

Keywords: Cu₄I₄ clusters; P,N-ligands; copper(I) complexes; phosphines; luminescent complexes



Citation: Enikeeva, K.R.; Shamsieva, A.V.; Strelnik, A.G.; Fayzullin, R.R.; Zakharychev, D.V.; Kolesnikov, I.E.; Dayanova, I.R.; Gerasimova, T.P.; Strelnik, I.D.; Musina, E.I.; et al. Green Emissive Copper(I)

Coordination Polymer Supported by the Diethylpyridylphosphine Ligand as a Luminescent Sensor for Overheating Processes. *Molecules* **2023**, *28*, 706. <https://doi.org/10.3390/molecules28020706>

Academic Editor: Yungen Liu

Received: 28 December 2022

Revised: 7 January 2023

Accepted: 8 January 2023

Published: 10 January 2023



Copyright: © 2023 by the authors. Licensee MDPI, Basel, Switzerland. This article is an open access article distributed under the terms and conditions of the Creative Commons Attribution (CC BY) license (<https://creativecommons.org/licenses/by/4.0/>).

1. Introduction

Designing luminescent copper(I) complexes is one of the current fields of interest in modern coordination chemistry; this is strongly motivated by the low cost and toxicity and the high availability of copper, relative to the noble and rare earth metals [1–6]. Copper(I) complexes are a large family of coordination compounds, displaying a variety of structures that depend on the denticity and bridging ability of the supporting ligands and counter ions [7–15].

Usually, the copper(I) halides form di- or tetranuclear clusters with the μ^2 -, μ^3 - or μ^4 - bridging coordination of halogen ions [9,10]. The tetranuclear copper(I) complexes are presented by clusters with three types of copper-halide cores (Figure 1): cubane-type [8,16–23], octahedral [17,24–31], and stairstep [32–38].

The complexes with cubane-type clusters are the most studied representatives of the tetranuclear complexes, which display dual-emission behavior with high sensitivity to temperature changes [8,16,21,23,39]. This type of complex has an L₄Cu₄X₄ composition (where L is a P-, N-, S- or other monodentate ligand). The octahedral and stairstep types of the tetranuclear complexes have an L₂Cu₄X₄ composition (where L is a bidentate ligand) [24,25,40]. The division into the octahedral and stairstep classes of complexes is

based on the geometry differences of the Cu_4X_4 cores, which can be found in the bridging coordination of the iodide ions and $\text{Cu} \cdots \text{Cu}$ distances. The octahedral clusters consist of a square-bipyramid formed by the four $\text{Cu}(\text{I})$ ions as the base of a bipyramid bounded by the two μ^4 -iodide ions as the apexes, with two μ^2 -iodide ions and two μ^2 -bidentate ligands lying in the one plane with a Cu_4 -core. The structure of the staircase-type core is determined by a zigzag chain, alternating the copper(I) and μ^3 -coordinated iodide links. In this type of cluster, the four copper(I) ions form a plane supported by the two μ^3 -iodide ions, two μ^2 -iodide ions, and two μ^2 -bidentate ligands. The μ^3 - or μ^4 -coordination of iodide ions is determined by the distance between two copper(I) ions at the core, which is commonly less than the sum of the van der Waals radii in the octahedral clusters (in the range of ca. 2.6–3.0 Å) and more than 3.0 Å in the staircase types of clusters [17,25,27,34,36].

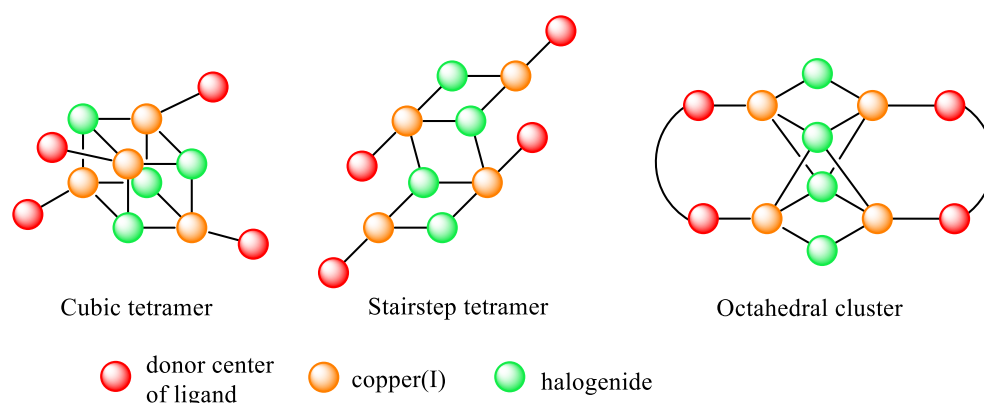


Figure 1. Schematic representation of three types of Cu_4X_4 clusters.

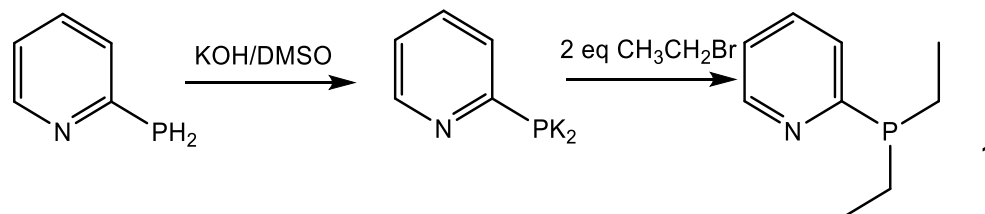
These differences contribute to the differences in the photophysical properties of the two types of complexes. The octahedral types of complexes often demonstrate dual-band emission in the high-energy (blue or green emission) and low-energy (red emission) ranges of the visible spectra. This phenomenon is attributed to emissions from two excited states, with the $^3(\text{M}+\text{X})\text{LCT}$ (metal–halide to ligand charge transfer) or ^3CC (cluster-centered) origins of transitions [29,31,40,41]. Those complexes with the staircase type of Cu_4X_4 core are able to emit in the full range of spectra; the energy of the emission depends on the chromophore groups contributing to the $^3(\text{M}+\text{X})\text{LCT}$ transitions of the complexes. To the best of our knowledge, there are no examples of staircase complexes displaying dual-emission behavior.

The tetranuclear octahedral and stair-step structural motifs generally require stabilization by the bidentate ligands (e.g., P,P- , N,N- or P,N- donor ligands). The copper(I) clusters with P,N- ligands are one of the most studied forms compared with clusters formed with other ligands [25,28,31]. Recently, we have demonstrated that the dual emission of octahedral clusters can be processed by the two excited states, with various distortions of the Cu_4I_4 core, which affects the energy of the $^3(\text{M}+\text{X})\text{LCT}$ transitions [29,42]. Moreover, the utilization of these conformationally restricted ligands allowed isolating clusters with two types of distortions of the Cu_4I_4 core, which demonstrates individual green or red emissions. This allowed the researchers to attribute the origin of the emissions of both octahedral clusters to $^3(\text{M}+\text{X})\text{LCT}$ transitions [42].

The rich photophysical properties of the copper(I) complexes with various ligands, including an intriguing dual emission, and the new findings of core distortions in complexes with conformationally restricted P,N- ligands motivated us to synthesize the sterically tiny diethylpyridylphosphine and study its complexation toward copper(I) iodide. Instead of the formation of a $\text{Cu}_4\text{I}_4\text{L}_2$ complex, a one-dimensional coordination polymer with the $\text{Cu}_4\text{I}_4\text{L}_2$ structural building unit was obtained. Its structure and photophysical properties are presented in this work.

2. Results

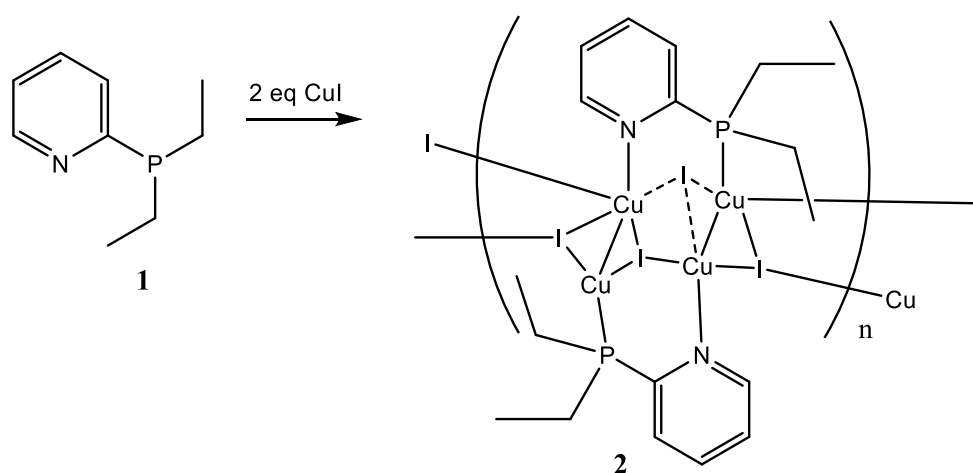
The diethylpyridylphosphine **1** was obtained via a two-step reaction, starting with primary phosphine PyPH₂, according to Scheme 1 by the previously reported procedure [43].



Scheme 1. Synthesis of diethyl-1-(pyridine-2-yl)phosphine.

The obtained phosphine is characterized by a one-septet signal, which is registered at -10.9 ppm ($^2J_{\text{PH}}$ 14.7 Hz) in the ^{31}P NMR spectrum. The position of signals, their multiplicity, and relative intensity in the ^1H NMR spectrum fully correspond to diethylpyridylphosphine [43].

The reaction of phosphine **1** with copper(I) iodide in the 1:2 metal-to-ligand ratio in dichloromethane (Scheme 2) leads to the formation of a yellowish crystalline precipitate, which represents the copper(I) polymer according to the X-ray diffraction (XRD) study.



Scheme 2. Synthesis of coordination polymer **2**.

According to the single-crystal XRD, complex **2** is a double polymeric chain that alternates the copper- and μ^3 -coordinated iodide links (Figure 2). The polymer chain is formed along the shortest axis, $0a$, of the unit cell ($P2_1/n$). The powder XRD pattern of polycrystalline sample **2** (Figure 3) demonstrates good agreement with the single-crystal XRD data and provides evidence of the homogeneity of the sample that is analyzed. One monomeric unit contains the stairstep centrosymmetric Cu_4I_4 core, supported by two diethylpyridylphosphine ligands. The monomeric unit can be described as a tetranuclear $\text{L}_2\text{Cu}_4\text{I}_4$ cluster (Figure 2). In the monomeric unit of the polymer, all the copper(I) ions exist in the tetrahedral geometry of the ligand environment, with the coordination of P–Cu or N–Cu bonds and three Cu–I bonds, where the iodide ions display bridging coordination.

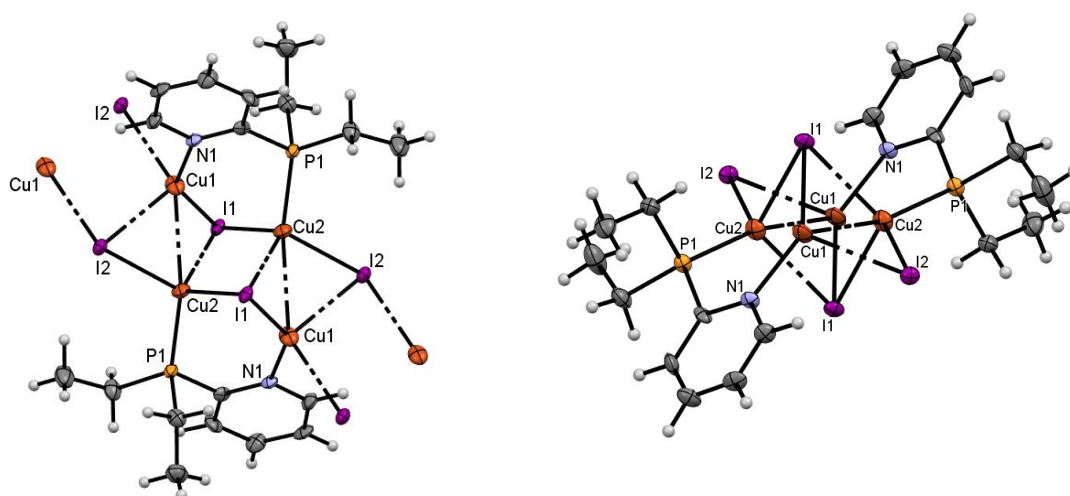


Figure 2. The structure of coordination polymer 2, shown in two projections.

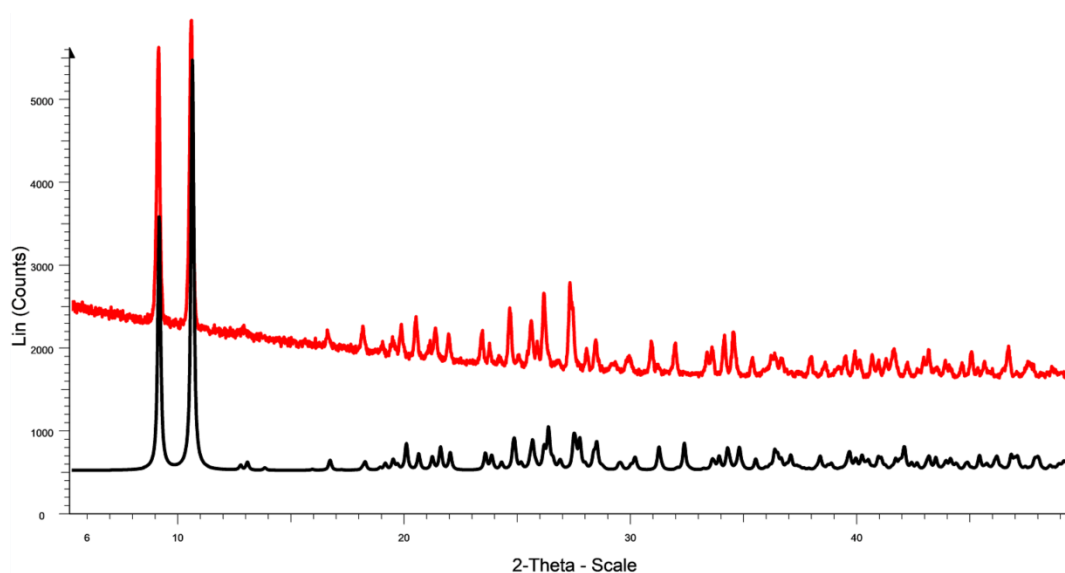


Figure 3. The theoretical powder diffractogram (black curve), calculated from single X-ray data for compound 2, and the experimental powder diffractograms of the polycrystalline sample (red curve).

All the copper(I) cations in the Cu_4 cluster of the monomeric unit lie on one plane, with the value of the distance between the neighboring copper(I) ions being 2.7693(14) and 3.0662(15) Å. Thus, the centrosymmetric Cu_4 -cluster exists as a parallelogram, with angle values of 63.95(4) and 116.05(4)°. The two molecules of pyridyl(diethyl)phosphines are coordinated to the Cu_4I_4 core via the P- and N-donor atoms in a head-to-tail manner. The Cu1 and I2 ions are bound by the iodide and copper(I) ions of the further monomeric units; this connectivity forms the continuous chain of the polymer. Furthermore, the chains in the crystal lie in plains parallel to $0ac$, and stack along the longest axis, $0b$, forming the layer-by-layer structure of the crystal with a packing index of 68.2%.

Notably, the stair-step structure of the Cu_4I_4 core can be presented as the distorted octahedral Cu_4I_4 core, when seen from the other viewpoint (Figure 2). The differences in the structure of the coordination polymer 2 and the published Cu_4I_4 octahedral structures lie in the greater distances between the Cu1 and Cu2 ions (3.066 Å in 2, versus ca. 2.7–2.9 Å in the octahedral clusters), the μ^3 -coordination mode of the I1 ions, and the deviation of the I2-ions from the Cu_4 plane in coordination polymer 2. Possibly, the distortion in the structure of 2 is caused by the polymeric assembly; such an arrangement is possible

due to the absence of the steric hindrance of the P,N-ligand. Conversely, some movement inside the Cu_4I_4 cluster might enable the formation of an octahedral cluster unit. Moreover, the monomeric unit of **2** turns out to be the average structure between the staircase and octahedral motifs; therefore, we should take into account in later works that the staircase and octahedral clusters might be the frontier cases of one structural motif, and, possibly, conversion between clusters can be observed.

The obtained polymer is slightly soluble in dichloromethane, acetone, acetonitrile, and DMF, while the dissolution of complex **2** in the DMSO leads to the oxidation of copper(I) to copper(II). The ^{31}P NMR spectra display a sharp signal at -1.4 ppm. The shift of the signal in the ^{31}P NMR ($\Delta\delta_{\text{P}}$ ca. 10 ppm) spectrum is close to that of the previously studied octahedral complexes [40,42]. The ^1H NMR indicates a slight broadening of the signals relative to the ligand signals, which is to be expected for the copper(I) complexes due to the shielding of the protons by the transition metal cation. The signals of the pyridyl and ethyl protons of the complex are strongly downfield-shifted relative to those of **1** ($\Delta\delta \approx 0.5\text{--}1$ ppm), which indicates the preservation of the N(Py)–Cu and P–Cu coordination bonds of the complex in solution.

With the aim of understanding the ability of complex **2** to retain its polymeric structure and establish its approximate stoichiometry in solution, diffusion NMR spectroscopy was used. According to the Stokes–Einstein model, the diffusion coefficient for a molecule is inversely proportional to the hydrodynamic molecular radius [44–47]. The complexes of smaller size and weight should exhibit different diffusion coefficients (SDCs) compared to the polymeric or oligomeric structures, which possess a larger size and weight. Thus a comparison was made for three samples in the DMF- d_7 solution (Table 1): ligand **1**, complex **2**, and the previously synthesized octahedral copper(I) iodide cluster $\text{L}_2\text{Cu}_4\text{I}_4$ (L is 1-(pyridine-2-yl)phospholane), acting as a reference compound with a predetermined structure [40].

Table 1. The self-diffusion coefficients and hydrodynamic radii of ligand **1**, complex **2**, and reference $\text{L}_2\text{Cu}_4\text{I}_4$.

Compound	Self-Diffusion Coefficient ¹ (10^{-9} m ² /s)	Hydrodynamic Radii r_{H} (Å)
Ligand 1	0.90	3.22
Complex 2	0.45	6.44
$\text{L}_2\text{Cu}_4\text{I}_4$	0.41	7.07

¹ DMF SDC is $1.10\text{--}1.43 \times 10^{-9}$ m²/s, depending on the sample, and r_{H} is 0.2 Å.

According to the determined self-diffusion coefficients, it can be concluded that the structures of complex **2** and the reference compound, $\text{L}_2\text{Cu}_4\text{I}_4$, have similar molecular volume; therefore, complex **2** does not retain a polymeric or even oligomeric structure in solution but exists as a molecular compound in solution. According to the shifting of the signals of phosphorus atoms and pyridyl protons, it is possible to suggest that the complex partially retains the structural motif with the P–Cu and N–Cu coordination bonds. The existence of sample **2** as a molecular complex in a solution is also supported by the ESI mass spectra of complex **2**, which indicates the presence of the peaks of the cations with $[2\text{L}+3\text{Cu}+2\text{I}]^+$, $[2\text{L}+2\text{Cu}+\text{I}]^+$, and $[2\text{L}+\text{Cu}]^+$ composition. The analogous fragmentation seen in the ESI mass spectrometry was observed earlier for the copper(I) complexes with the octahedral Cu_4I_4 structure of the copper-halide core [29,42].

Complex **2** or its parts is not emissive in the solution but displays moderate emission in the solid state (Figure 4a). The emission spectrum is represented by a band with a maximum of 505 nm, while the excitation spectrum displays a broad band with a maximum in the region of 356–380 nm. The emission of complex **2** displays a dual exponential luminescence decay, with 0.64 and 2.5 μs lifetimes. The large Stokes shift (ca. 8000 cm^{-1}) and the microsecond domain of the lifetimes indicate the phosphorescent origin of the emission. The luminescence quantum yield of complex **2** in the solid state (20%) is rather high in comparison with that of the other representatives of the polymeric copper(I) complexes.

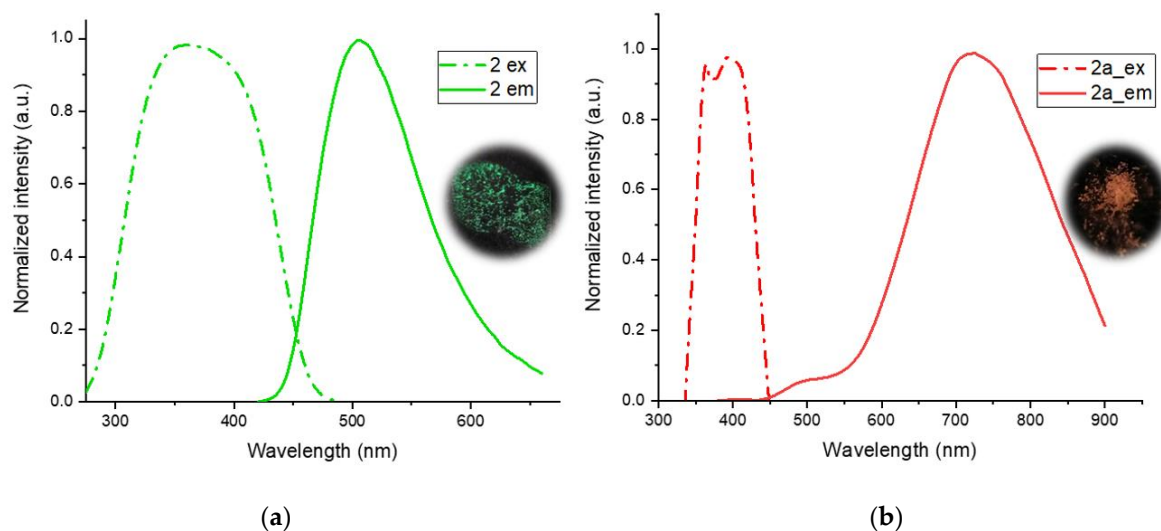


Figure 4. Solid-state excitation (dash-dot) and the emission (solid) spectra of polymer **2** (a) and solid phase **2a**; (b) powders of polymer **2** and solid phase **2a** under UV-light irradiation (365 nm).

The heating up of the coordination polymer **2** to 138.5 °C leads to a change in the color of the sample emission to red, with the maximum at 725 nm in the emission spectra, although the cooling-down of the sample to room temperature does not mark a return to green emission conditions. Thus, the heating up of sample **2** leads to the solid-state transformation of the polymer to the solid phase **2a**, which was confirmed by differential scanning calorimetry (DSC) (Figure 5).

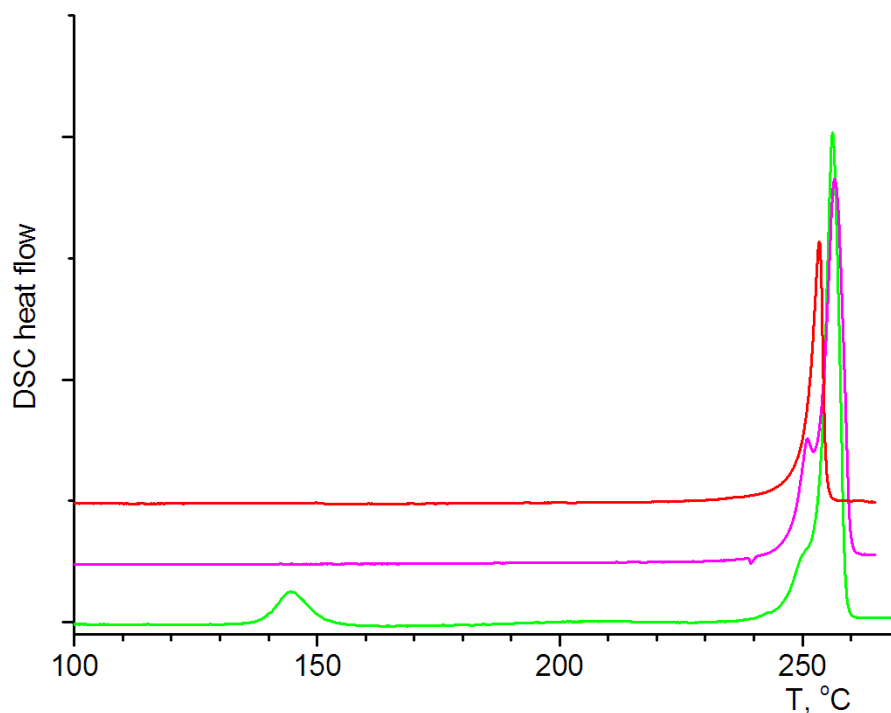


Figure 5. The DSC curves of polymer **2** in the direct mode (green line), of the crystallized melt sample rescan mode (pink line), and of the solid phase **2a** (red line).

According to the DSC, the solid-state transformation of polymer **2** into polymer **2a** occurred at 138.2 °C (endothermic peak) without the decomposition of the sample. Further melting, as a complex endothermic event, was observed at 251.7 °C. The rescan of the

sample, obtained after crystallization of the melt, displays the absence of pronounced thermal events until its melting. Thus, for the green-emissive sample **2**, the transformation to another crystalline phase, **2a**, occurs within the DSC experiment, which is accessible upon returning to room-temperature conditions. The crystalline phase, **2a**, which was prepared by heating polymer **2** up to 140 °C and annealing for 15 min, displays the same thermal characteristics as the sample in the rescan experiment. The solid-state phase, **2a**, can be converted back to polymer **2** via recrystallization, from either the DMF or acetone solutions. Therefore, the obtained coordination polymer **2** can be considered to be a sensor and can be applied in the detection of overheating in those processes that should take place at temperatures below 138 °C (e.g., engines, boiling liquids, solar heating systems, etc.).

According to the DSC, NMR, and photophysical experiments, it is possible to suggest that polymer **2** does not retain its polymeric structure during heating to 138.2 °C; instead, it transforms into a molecular complex, **2a**, which displays a red emission. Moreover, our recent studies of the Cu₄I₄-octahedral complexes demonstrated that such a type of complex is able to demonstrate both green and red emissions, which are caused by the ³(M+X)LCT transition of those structures with different symmetry from the copper-halide core [23,34]. According to the XRD data, the monomeric unit of polymer **2** can be regarded as a distorted octahedral Cu₄I₄-complex; consequently, the heating of polymer **2** probably leads to the “concerted” movement of the copper(I) and iodide, which, in turn, could result in the formation of the molecular complex **2a** with an octahedral Cu₄I₄ core.

To evaluate the influence of polymer formation on the compound’s photophysical properties, compound **2** was considered in the same way as the monomeric and dimeric molecules within quantum chemical computations (Figure 6). During the optimization of the monomeric unit, the copper-halide core structure transformed from a staircase into octahedral geometry; at the same time, the central copper-halide fragment in the dimeric model retained its initial staircase geometry, whereas the peripheral Cu and I atoms tended to adopt an octahedral geometry (Figure 6).

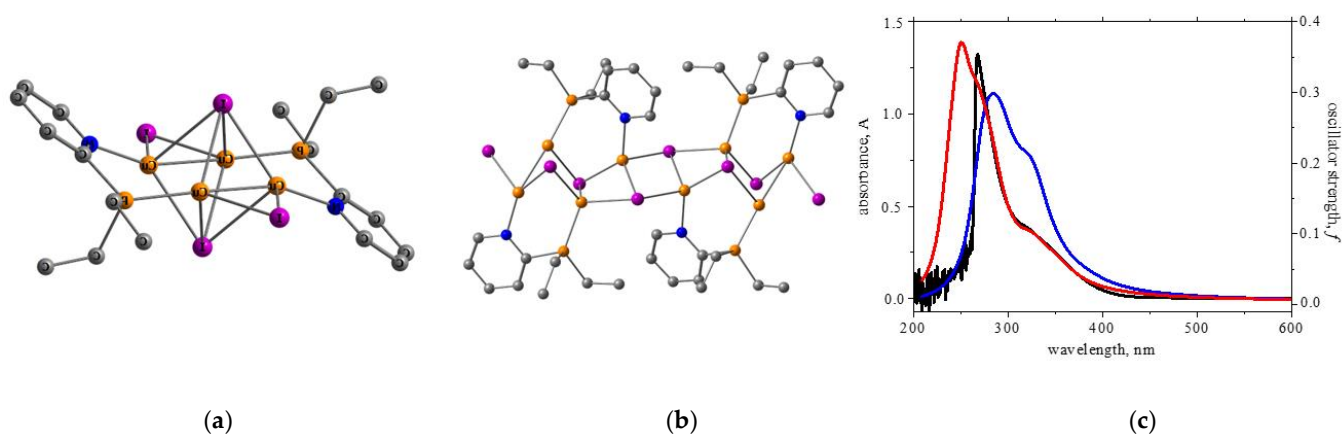


Figure 6. Quantum-chemically optimized monomeric (a) and dimeric (b) models of polymer **2** (orange—Cu atoms, pink—I atoms, blue—N atoms, grey—C atoms); (c) the simulated UV/Vis spectra for the monomeric (red line) and dimeric (blue line) models, compared to the experimental (black line) spectrum of polymer **2**.

The predicted UV/Vis spectrum for the monomeric model is slightly blue-shifted, compared to the one predicted for a dimer (Figure 6c), and better matches the experimental curve, suggesting the presence of monomeric units in the solution rather than a polymer structure [48,49]. At the same time, the computations predict a T₁-S₀ transition (Figure 7) for the monomer in a lower energy range (464 nm) compared to the dimer (437 nm).

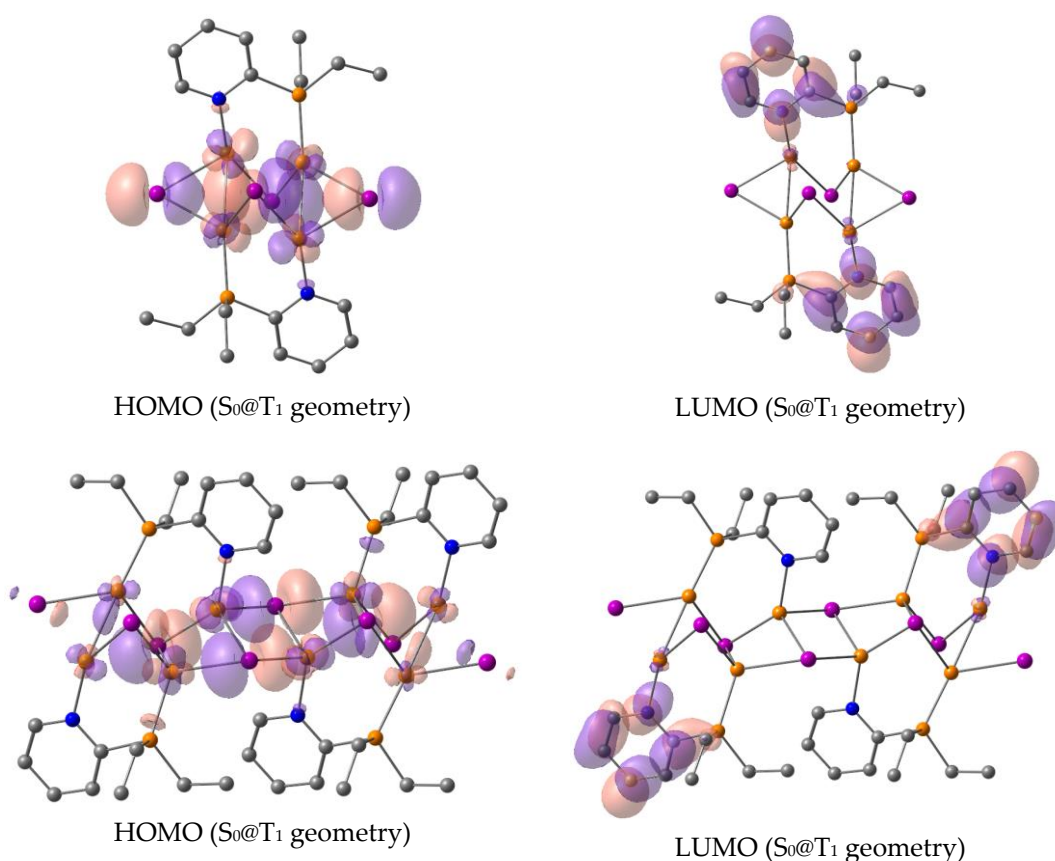


Figure 7. Frontier orbitals of the singlet ground states (S_0) for the optimized T_1 ($S_0@T_1$) geometries of the monomer (top) and dimer (bottom) models (orange—Cu atoms, pink—I atoms, blue—N atoms, grey—C atoms).

Therefore, the agreement of the quantum chemical calculations with the UV/vis-absorption spectra, the tendency found in the predicted energies of the T_1 - S_0 transitions, and the thermochemical behavior, as well as the NMR spectroscopic and mass-spectrometric studies of the solutions of **2**, support our assumption that the staircase structure of polymer **2** is able to transform into a molecular complex with an octahedral copper(I)-halide core when heated up to 138.2 °C.

3. Materials and Methods

All reactions and purification manipulations were carried out under a dry argon atmosphere, using standard vacuum-line techniques. Commercially available solvents were purified, dried, deoxygenated, and distilled before use. Primary phosphine PyPH₂ was obtained using the standard method described by Redmore [50].

The ¹H NMR (400.13 MHz) and ³¹P NMR (161.96 MHz) spectra were recorded on a Bruker Avance 400 spectrometer (Karlsruhe, Germany), using the residual solvent as an internal reference for ¹H ($\delta = 7.26$ in CDCl₃, and $\delta = 5.31$ ppm in CD₂Cl₂) and 85% aqueous solution of H₃PO₄ as an external reference for ³¹P. The chemical shifts are reported in ppm and coupling constants (J) are reported in Hz.

The DOSY NMR experiments were performed on a Bruker AVANCE-500 spectrometer (Karlsruhe, Germany). The spectrometer was equipped with a Bruker multinuclear z-gradient inverse probe head that is capable of producing gradients with a strength of 50 G cm⁻¹. All experiments were carried out at 303 ± 0.2 K. Chemical shifts (δ) were reported relative to DMF (2.900 ppm for an upfield peak of the CH₃ group) as an internal standard. To prevent convection in the diffusion NMR spectroscopy experiments, the test sample was loaded into a thin-walled glass 3-millimeter NMR tube and then inserted into

the standard 5-millimeter tube usually employed for NMR experiments. The capacity between these tubes was filled up with a solvent DMF- d_7 . After Fourier transformation and baseline correction, the diffusion dimension was processed with the Bruker TopSpin software package (version 3.2). The diffusion constants were calculated by the exponential fitting of the data, belonging to individual columns of the pseudo-2D matrix. Single components have been assumed for the fitting routine. All separated peaks were analyzed and the average values were presented. Hydrodynamic radii (R_H) were calculated from the self-diffusion coefficient D_s , applying the Stokes–Einstein equation: $D_s = kT/6\pi\eta R_H$, where k is the Boltzmann constant ($1.38 \times 10^{-23} \text{ JK}^{-1}$), T is the absolute temperature (303 K), and η (DMF, 303 K) = $7.66 \times 10^{-4} \text{ Pa}$ is the viscosity of the solvent.

ESI measurements were performed using an AmaZon X ion-trap mass spectrometer (Bremen, Germany) in both positive and negative modes. The mass spectra are given as m/z values and relative intensities (I_{rel} , %). Chloroform and dimethylformamide were used as solvents for the mass spectrometry measurements.

Elemental analysis was carried out on a EuroVector-3000 (Pavia, Italy). The determination of the phosphorus and copper content was provided by combustion in an oxygen stream, whereas the content of iodine was found using the Scheniger method.

Differential scanning calorimetry (DSC) was carried out on a Netzsch DSC 204 F1 Phoenix calorimeter (τ -sensor) (Hanau, Germany) using cold-welded aluminum cells in the temperature range of 20–110 °C at a scanning rate of 5 °C/min⁻¹. To take sample portions, a Sartorius CPA-2P microbalance was used; the weight of the sample was 1–3 mg.

Powder X-ray diffraction. Powder XRD experiments were performed on a Bruker D8 Advance diffractometer (Karlsruhe, Germany) equipped with a Vario setup and a Vantec linear detector. $\text{CuK}\alpha_1$ radiation, monochromated by a Johansson monochromator, was used for the test. Experiments were performed at room temperature in the Bragg–Brentano geometry with a planar sample. Powder samples were placed on the surface of a single-crystalline silicon plate.

Single-crystal XRD analysis. An X-ray diffraction study of **2** was performed on a Bruker KAPPA APEX II diffractometer (Karlsruhe, Germany). The data collected were processed using the APEX4 software. The structure was solved by the direct method, using the SHELXT program [51], and then refined by the full-matrix least-squares method on F^2 , using the SHELXL program [52]. Non-hydrogen atoms were refined in the anisotropic approximation. The hydrogen atoms were inserted at geometrically calculated positions and were included in the refinement as riding atoms.

Deposition number CCDC 2225852 contains the supplementary crystallographic data for compound **2**. These data are provided free of charge by the joint Cambridge Crystallographic Data Centre and the Fachinformationszentrum Karlsruhe Access Structures service www.ccdc.cam.ac.uk/structures (accessed on 27 December 2022).

Crystallographic data for 2: $\text{C}_9\text{H}_{14}\text{Cu}_2\text{I}_2\text{NP}$, colorless prism ($0.425 \times 0.169 \times 0.119 \text{ mm}^3$), formula weight 548.06 g mol^{-1} ; monoclinic, $P2_1/n$ (No. 14), $a = 7.7606(6) \text{ \AA}$, $b = 19.4506(17) \text{ \AA}$, $c = 9.6518(8) \text{ \AA}$, $\beta = 106.079(3)^\circ$, $V = 1399.9(2) \text{ \AA}^3$, $Z = 4$, $T = 173(2) \text{ K}$, $d_{\text{calc}} = 2.600 \text{ g cm}^{-3}$, $\mu(\text{Mo K}\alpha) = 7.532 \text{ mm}^{-1}$, $F(000) = 1016$; $T_{\text{max/min}} = 0.1848/0.0712$; 31,014 reflections were collected ($2.926^\circ \leq \theta \leq 27.976^\circ$, index ranges: $-10 \leq h \leq 10$, $-25 \leq k \leq 25$, and $-11 \leq l \leq 12$), 3312 of which were unique, $R_{\text{int}} = 0.0547$, $R_\sigma = 0.0388$; completeness to θ of 27.976° 98.3%. The refinement of 138 parameters with no restraints converged to $R1 = 0.0475$ and $wR2 = 0.1340$ for 2781 reflections with $I > 2\sigma(I)$ and $R1 = 0.0590$ and $wR2 = 0.1436$ for all data with a goodness-of-fit of $S = 1.114$ and residual electron density $\rho_{\text{max/min}} = 2.508$ and $-1.579 \text{ e \AA}^{-3}$, RMS 0.337; max shift/e.s.d. in the last cycle, 0.001.

Photophysical measurements: UV-Vis spectra were registered at room temperature on a Perkin-Elmer Lambda 35 spectrometer (Rodgau, Germany) with a scan speed of 480 nm min^{-1} , using a spectral width of 1 nm. The sample of compound **2** was prepared as a solution in DMF with a concentration of $1.1 \times 10^{-4} \text{ mol}\cdot\text{L}^{-1}$ and then placed in 10 mm quartz cells. The photoluminescence properties of the solid-state samples at room temperature were measured on a Fluorolog-3 (Horiba Jobin Yvon, Bensheim, Germany)

spectrofluorometer. The powder samples were supported on the quartz glass plates. LED testing ($\lambda_{\text{ex}} = 370$ nm) was used to carry out lifetime measurements (pulse width 1 ns, and repetition rate 100 kHz). The integration sphere (Quanta- ϕ , 6 inches) was used to measure the solid-state emission quantum yield. The measurements were carried out with powders, according to the guide provided by the manufacturer (four spectra-based measurements).

Computational methods: Quantum chemical calculations were performed with the Gaussian 16 (Revision A) [53] suite of programs. The ground/excited-state structures were optimized with the use of the hybrid PBE0 functional [54] model and the Ahlrichs' triple- ζ def-TZVP AO basis set [55]. In all geometry optimizations, the D3 approach [56], used to describe the London dispersion interactions, together with the Becke–Johnson damping function [57–59], were employed as implemented in the Gaussian 16 program. A time-dependent density functional response theory (TDDFT) with the use of CAM-B3LYP [60] (functional) has been employed to compute the vertical excitation energies (i.e., absorption wavelengths) and oscillator strengths for the ground-state optimized geometries in the gas phase, where the 50 lowest singlet excited states were taken into account. The vertical T_1 - S_0 transition energies were also computed, using the TDDFT approach at the CAM-B3LYP/def-TZVP level, for the triplet geometries optimized by the UPBE0–D3(BJ)/def-TZVP level of theory. The calculated spectra were shifted by -0.24 eV.

Synthesis of ligand 1: Diethylpyridylphosphine **1** was obtained via the previously reported procedure [43].

To a solution of pyridine-2-ylphosphine (19 mmol) in DMSO (35 mL), a 56% aqueous solution of KOH (57 mmol) was added, and the reaction mixture became red-colored. After 2 h, the reaction mixture was cooled to 5 °C, and a solution of bromoethane (38 mmol) in DMSO (25 mL) was added dropwise over 30 min. The mixture was held at room temperature and stirred overnight. Degassed water (30 mL) was added, then the organic layer was separated via a cannula, and residuary products were extracted with n-hexane (3×40 mL) from the aqueous layer. The organic layer was dried over MgSO_4 . The solvent was removed by distillation; the residue was separated by fractional distillation under reduced pressure. Yield 0.72 g (23%). b.p. 47 °C/0.02 mbar. ^1H NMR (CDCl_3): δ_{H} 8.50 (d, $^3J_{\text{HH}} = 4.7$ Hz, 1H, Py), 7.43 (ddd, $^4J_{\text{HH}} = 1.9$ Hz, $^3J_{\text{HH}} = ^3J_{\text{HH}} = 4.8$ Hz, 1H, Py), 7.29 (m, 1H, Py), 6.98 (ddd, $^3J_{\text{HH}} = 6.2$ Hz, $^3J_{\text{HH}} = 4.9$ Hz, $^4J_{\text{HH}} = 2.6$ Hz, 1H, Py), 1.73 (q, $^2J_{\text{HH}} = 15.3$ Hz, $^3J_{\text{HH}} \approx 7.6$ Hz, 2H, $-\text{CH}_{2\text{A}}-$), 1.61 (q, $^2J_{\text{HH}} = 15.3$ Hz, $^3J_{\text{HH}} \approx 7.6$ Hz, 2H, $-\text{CH}_{2\text{B}}-$), 0.9 (ddd, $^3J_{\text{HH}} \approx ^3J_{\text{HH}} \approx 7.6$ Hz, $^3J_{\text{PH}} \approx 15.0$ Hz, 6H, $-\text{CH}_3$). ^{31}P NMR (CDCl_3): $\delta_{\text{P}} -10.9$ ppm.

Synthesis of Complex 2: To a solution of **1** (0.3 g, 1.79 mmol) in dichloromethane (3 mL), the suspension of copper (I) iodide (0.68 g, 3.59 mmol) in dichloromethane (5 mL) was added. The color of the reaction mixture changed from colorless to yellow, and precipitation of the product was observed. The reaction mixture was stirred for 12 h at room temperature. Afterward, a yellowish precipitate was filtered off, washed with dichloromethane, and dried under a vacuum. Yield: 0.57 g (58%); mp = 136 °C. NMR ^1H (400 MHz, CD_2Cl_2): δ_{H} 8.71 (d, $^3J_{\text{HH}} = 4.9$ Hz, 1H, H-Py), 7.66 (m, 1H, H-Py), 7.64 (dddd, $^3J_{\text{HH}} \approx ^3J_{\text{HH}} \approx 7.3$, $^4J_{\text{HH}} \approx ^4J_{\text{PH}} \approx 2$ Hz, 1H, H-Py), 7.23 (dddd, $^3J_{\text{HH}} = 4.9$, $^3J_{\text{HH}} = 7.3$, $^4J_{\text{HH}} \approx ^5J_{\text{PH}} \approx 2$ Hz, 1H, H-Py), 2.21–2.29 (m, 2H, H-PCH₂), 2.11–2.20 (m, 2H, PCH₂), 1.78–1.87 (m, 4H, H-CH₃). ^{31}P NMR (CD_2Cl_2) $\delta_{\text{P}} -8.4$ (br.s). MS (ESI_{pos}, m/z (I_{rel} , %), ion): 748 (51) [$3\text{L} + 2\text{Cu} + \text{I}$]⁺, 584 (63) [$2\text{L} + 2\text{Cu} + \text{I}$]⁺, 393 (100) [$2\text{L} + \text{Cu}$]⁺. Anal. Calcd. for $\text{C}_{26}\text{H}_{35}\text{N}_3\text{P}_3\text{Cu}_2\text{I}_2$: C, 37.00; H, 4.14; Cu, 14.50; I, 28.96; N, 4.79; P, 10.60%. Found: C, 36.95; H, 4.12; Cu, 14.52; I, 29.01; N, 4.74; P, 10.57%. Solid phase **2a** (red emitter). The obtained complex **2** (0.03 g) was heated up to 140 °C and annealed for 15 min to give pure phase **2a**. Reverse synthesis of polymer **2** (green emitter) from **2a**. The obtained complex **2a** (0.05 g) was dissolved in 2 mL of DMF. The solution was dropped onto the glass plate and left for 5 min at room temperature until the crystals formed.

4. Conclusions

In summary, it was demonstrated that diethylpyridylphosphine is able to form a copper(I) iodide complex with a polymeric structure and P,N-coordination of the ligand.

The new polymer is characterized by the intermediate structure, which can be assigned for both the staircase and octahedral types of copper halide clusters. Thus, it should be taken into account that staircase and octahedral clusters might not be individual, rigid cluster types but instead coordination isomers that can transform into one another. The studies of solutions of the polymer in question allowed us to demonstrate that the complex considered does not show the polymeric architecture in solutions, and the solvation of the polymer leads to its monomerization with the formation of the molecular complex. The obtained coordination polymer is the triplet emitter, which displays a green emission with a maximum of 505 nm. The heating of the polymer at 138.5 °C leads to its transformation to a new solid-state phase, which probably consists of the molecular complex with the octahedral structure of the copper-halide core. This assumption was supported by the quantum chemical study of the monomeric unit of the polymer. The recrystallization of the new solid phase from acetone or DMF returns the crystalline sample of the polymer. Therefore, the polymer can be considered to be a sensor for detecting the overheating of materials over 138 °C.

Author Contributions: Conceptualization, I.D.S., E.I.M. and A.A.K.; methodology, A.V.S., A.G.S., D.V.Z., I.E.K., R.R.F., T.P.G. and K.R.E.; formal analysis, A.V.S., A.G.S. and I.D.S.; investigation, K.R.E., A.V.S., A.G.S., R.R.F., D.V.Z., I.E.K., I.R.D. and T.P.G.; writing—original draft preparation, A.V.S., R.R.F., A.G.S., T.P.G. and I.D.S.; writing—review and editing, I.D.S., E.I.M., A.A.K. and O.G.S.; supervision, A.A.K. and O.G.S.; project administration, O.G.S. All authors have read and agreed to the published version of the manuscript.

Funding: This research was funded by the Russian Science Foundation, grant number 19-13-00163-P.

Institutional Review Board Statement: Not applicable.

Informed Consent Statement: Not applicable.

Data Availability Statement: Cambridge Crystallographic Data Centre #2225852.

Acknowledgments: The physical experiments were carried out on the equipment of the Assigned Spectral-Analytical Center of FRC Kazan Scientific Center of RAS and the Centre for Optical and Laser Materials Research of Saint Petersburg State University Research Park.

Conflicts of Interest: The authors declare no conflict of interest.

References

1. Troyano, J.; Zamora, F.; Delgado, S. Copper(I)–Iodide Cluster Structures as Functional and Processable Platform Materials. *Chem. Soc. Rev.* **2021**, *50*, 4606–4628. [[CrossRef](#)]
2. Wenger, O.S. Vapochromism in Organometallic and Coordination Complexes: Chemical Sensors for Volatile Organic Compounds. *Chem. Rev.* **2013**, *113*, 3686–3733. [[CrossRef](#)] [[PubMed](#)]
3. Czerwieniec, R.; Leitl, M.J.; Homeier, H.H.H.; Yersin, H. Cu(I) Complexes—Thermally Activated Delayed Fluorescence. Photo-physical Approach and Material Design. *Coord. Chem. Rev.* **2016**, *325*, 2–28. [[CrossRef](#)]
4. Cariati, E.; Lucenti, E.; Botta, C.; Giovanella, U.; Marinotto, D.; Righetto, S. Cu(I) Hybrid Inorganic–Organic Materials with Intriguing Stimuli Responsive and Optoelectronic Properties. *Coord. Chem. Rev.* **2016**, *306*, 566–614. [[CrossRef](#)]
5. Hei, X.; Liu, W.; Zhu, K.; Teat, S.J.; Jensen, S.; Li, M.; O’Carroll, D.M.; Wei, K.; Tan, K.; Cotlet, M.; et al. Blending Ionic and Coordinate Bonds in Hybrid Semiconductor Materials: A General Approach toward Robust and Solution-Processable Covalent/Coordinate Network Structures. *J. Am. Chem. Soc.* **2020**, *142*, 4242–4253. [[CrossRef](#)] [[PubMed](#)]
6. Liu, W.; Fang, Y.; Li, J. Copper Iodide Based Hybrid Phosphors for Energy-Efficient General Lighting Technologies. *Adv. Funct. Mater.* **2018**, *28*, 1705593. [[CrossRef](#)]
7. Tsuge, K.; Chishina, Y.; Hashiguchi, H.; Sasaki, Y.; Kato, M.; Ishizaka, S.; Kitamura, N. Luminescent Copper(I) Complexes with Halogenido-Bridged Dimeric Core. *Coord. Chem. Rev.* **2016**, *306*, 636–651. [[CrossRef](#)]
8. Vitale, M.; Ford, P.C. Luminescent Mixed Ligand Copper(I) Clusters (CuI)_n(L)_m (L=pyridine, Piperidine): Thermodynamic Control of Molecular and Supramolecular Species. *Coord. Chem. Rev.* **2001**, *219–221*, 3–16. [[CrossRef](#)]
9. Peng, R.; Li, M.; Li, D. Copper(I) Halides: A Versatile Family in Coordination Chemistry and Crystal Engineering. *Coord. Chem. Rev.* **2010**, *254*, 1–18. [[CrossRef](#)]
10. Rong, M.K.; Holtrop, F.; Slootweg, J.C.; Lammertsma, K. Enlightening Developments in 1,3-P,N-Ligand-Stabilized Multinuclear Complexes: A Shift from Catalysis to Photoluminescence. *Coord. Chem. Rev.* **2019**, *382*, 57–68. [[CrossRef](#)]

11. Strel'nik, I.D.; Dayanova, I.R.; Kolesnikov, I.E.; Fayzullin, R.R.; Litvinov, I.A.; Samigullina, A.I.; Gerasimova, T.P.; Katsyuba, S.A.; Musina, E.I.; Karasik, A.A. The Assembly of Unique Hexanuclear Copper(I) Complexes with Effective White Luminescence. *Inorg. Chem.* **2019**, *58*, 1048–1057. [[CrossRef](#)]
12. Artem'ev, A.V.; Doronina, E.P.; Rakhmanova, M.I.; Tarasova, O.A.; Bagryanskaya, I.Y.; Nedolya, N.A. Chemoselective Mechanochemical Route toward a Bright TADF-Emitting CuI-Based Coordination Polymer. *Inorg. Chem. Front.* **2019**, *6*, 671–679. [[CrossRef](#)]
13. Vinogradova, K.A.; Plyusnin, V.F.; Kupryakov, A.S.; Rakhmanova, M.I.; Pervukhina, N.V.; Naumov, D.Y.; Sheludyakova, L.A.; Nikolaenkova, E.B.; Krivopalov, V.P.; Bushuev, M.B. Halide Impact on Emission of Mononuclear Copper(I) Complexes with Pyrazolylpyrimidine and Triphenylphosphine. *Dalton. Trans.* **2014**, *43*, 2953–2960. [[CrossRef](#)] [[PubMed](#)]
14. Baranov, A.Y.; Pritchina, E.A.; Berezin, A.S.; Samsonenko, D.G.; Fedin, V.P.; Belogorlova, N.A.; Gritsan, N.P.; Artem'ev, A.V. Beyond Classical Coordination Chemistry: The First Case of a Triply Bridging Phosphine Ligand. *Angew. Chem. Int. Ed.* **2021**, *60*, 12577–12584. [[CrossRef](#)] [[PubMed](#)]
15. Jin, J.-C.; Wang, J.; Guo, J.; Yan, M.-H.; Wang, J.; Srivastava, D.; Kumar, A.; Sakiyama, H.; Muddassir, M.; Pan, Y. A 3D Rare Cubane-like Tetramer Cu(II)-Based MOF with 4-Fold Dia Topology as an Efficient Photocatalyst for Dye Degradation. *Colloids Surf. A* **2023**, *656*, 130475. [[CrossRef](#)]
16. Nagaoka, S.; Ozawa, Y.; Toriumi, K.; Abe, M. A Dual-Emission Strategy for a Wide-Range Phosphorescent Color-Tuning of a Crystalline-State Molecular Cluster [Cu₄I₄(2-Bzpy)₄] (2-Bzpy = 2-Benzylpyridine). *Chem. Lett.* **2018**, *47*, 1101–1104. [[CrossRef](#)]
17. Neshat, A.; Aghakhanpour, R.B.; Mastroilli, P.; Todisco, S.; Molani, F.; Wojtczak, A. Dinuclear and Tetranuclear Copper(I) Iodide Complexes with P and P'N Donor Ligands: Structural and Photoluminescence Studies. *Polyhedron* **2018**, *154*, 217–228. [[CrossRef](#)]
18. Trivedi, M.; Singh, G.; Kumar, A.; Rath, N.P. Syntheses, Characterization, and Structural Studies of Copper(I) Complexes Containing 1,1'-Bis(Di-Tert-Butylphosphino)Ferrocene (Dtbbpf) and Their Application in Palladium-Catalyzed Sonogashira Coupling of Aryl Halides. *Dalton Trans.* **2014**, *43*, 13620–13629. [[CrossRef](#)]
19. Perruchas, S. Molecular Copper Iodide Clusters: A Distinguishing Family of Mechanochromic Luminescent Compounds. *Dalton Trans.* **2021**, *50*, 12031–12044. [[CrossRef](#)]
20. Kiracki, K.; Fejfarová, K.; Martinčík, J.; Nikl, M.; Lang, K. Tetranuclear Copper(I) Iodide Complexes: A New Class of X-ray Phosphors. *Inorg. Chem.* **2017**, *56*, 4609–4614. [[CrossRef](#)]
21. De Angelis, F.; Fantacci, S.; Sgamellotti, A.; Cariati, E.; Ugo, R.; Ford, P.C. Electronic Transitions Involved in the Absorption Spectrum and Dual Luminescence of Tetranuclear Cubane [Cu₄I₄(Pyridine)₄] Cluster: A Density Functional Theory/Time-Dependent Density Functional Theory Investigation. *Inorg. Chem.* **2006**, *45*, 10576–10584. [[CrossRef](#)] [[PubMed](#)]
22. Galimova, M.F.; Zueva, E.M.; Dobrynin, A.B.; Samigullina, A.I.; Musin, R.R.; Musina, E.I.; Karasik, A.A. Cu₄I₄-Cubane Clusters Based on 10-(Aryl)Phenoxarsines and Their Luminescence. *Dalton Trans.* **2020**, *49*, 482–491. [[CrossRef](#)]
23. Galimova, M.F.; Zueva, E.M.; Dobrynin, A.B.; Kolesnikov, I.E.; Musin, R.R.; Musina, E.I.; Karasik, A.A. Luminescent Cu₄I₄-Cubane Clusters Based on N-Methyl-5,10-Dihydrophenarsazines. *Dalton Trans.* **2021**, *50*, 13421–13429. [[CrossRef](#)] [[PubMed](#)]
24. Naik, S.; Mague, J.T.; Balakrishna, M.S. Short-Bite PNP Ligand-Supported Rare Tetranuclear [Cu₄I₄] Clusters: Structural and Photoluminescence Studies. *Inorg. Chem.* **2014**, *53*, 3864–3873. [[CrossRef](#)]
25. Liu, Z.; Djurovich, P.I.; Whited, M.T.; Thompson, M.E. Cu₄I₄ Clusters Supported by P'N-Type Ligands: New Structures with Tunable Emission Colors. *Inorg. Chem.* **2012**, *51*, 230–236. [[CrossRef](#)] [[PubMed](#)]
26. Wang, S.; Morgan, E.E.; Panuganti, S.; Mao, L.; Vishnoi, P.; Wu, G.; Liu, Q.; Kanatzidis, M.G.; Schaller, R.D.; Seshadri, R. Ligand Control of Structural Diversity in Luminescent Hybrid Copper(I) Iodides. *Chem. Mater.* **2022**, *34*, 3206–3216. [[CrossRef](#)]
27. Yadav, D.; Kumar Siwatch, R.; Sinhababu, S.; Karwasara, S.; Singh, D.; Rajaraman, G.; Nagendran, S.; Siwatch, R.K.; Sinhababu, S.; Karwasara, S.; et al. Digermylene Oxide Stabilized Group 11 Metal Iodide Complexes. *Inorg. Chem.* **2015**, *54*, 11067–11076. [[CrossRef](#)]
28. Chen, K.; Shearer, J.; Catalano, V.J. Subtle Modulation of Cu₄X₄L₂ Phosphine Cluster Cores Leads to Changes in Luminescence. *Inorg. Chem.* **2015**, *54*, 6245–6256. [[CrossRef](#)] [[PubMed](#)]
29. Shamsieva, A.V.; Kolesnikov, I.E.; Strel'nik, I.D.; Gerasimova, T.P.; Kalinichev, A.A.; Katsyuba, S.A.; Musina, E.I.; Lähderanta, E.; Karasik, A.; Sinyashin, O.G. Fresh Look on the Nature of Dual-Band Emission of Octahedral Copper-Iodide Clusters-Promising Ratiometric Luminescent Thermometers. *J. Phys. Chem. C* **2019**, *123*, 25863–25870. [[CrossRef](#)]
30. Emerson, E.W.; Cain, M.F.; Sanderson, M.D.; Knarr, C.B.; Glueck, D.S.; Ahern, J.C.; Patterson, H.E.; Rheingold, A.L. Synthesis, Structure, and Luminescence of the "Octahedral" Cluster Cu₄I₄(Rac-IsMePCH₂PMels)₂ (Is = 2,4,6-(i-Pr)₃C₆H₂). *Inorg. Chim. Acta.* **2015**, *427*, 168–172. [[CrossRef](#)]
31. Boden, P.; Di Martino-Fumo, P.; Busch, J.M.; Rehak, F.R.; Steiger, S.; Fuhr, O.; Nieger, M.; Volz, D.; Klopffer, W.; Bräse, S.; et al. Investigation of Luminescent Triplet States in Tetranuclear CuI Complexes: Thermochromism and Structural Characterization. *Chem.-A Eur. J.* **2021**, *27*, 5439–5452. [[CrossRef](#)] [[PubMed](#)]
32. Artem'ev, A.V.; Baranov, A.Y.; Rakhmanova, M.I.; Malysheva, S.F.; Samsonenko, D.G. Copper(I) Halide Polymers Derived from Tris[2-(Pyridin-2-Yl)Ethyl]Phosphine: Halogen-Tunable Colorful Luminescence Spanning from Deep Blue to Green. *New J. Chem.* **2020**, *44*, 6916–6922. [[CrossRef](#)]
33. Song, R.F.; Xie, Y.B.; Li, J.R.; Bu, X.H. Syntheses and Crystal Structures of the Copper(I) Complexes with Quinoline-Based Monothioether Ligands. *CrystEngComm* **2005**, *7*, 249–254. [[CrossRef](#)]

34. Yuan, S.; Liu, S.S.; Sun, D. Two Isomeric [Cu₄I₄] Luminophores: Solvothermal/Mechanochemical Syntheses, Structures and Thermochromic Luminescence Properties. *CrystEngComm* **2014**, *16*, 1927–1933. [[CrossRef](#)]
35. Bai, S.Q.; Jiang, L.; Young, D.J.; Hor, T.S.A. Luminescent [Cu₄I₄] Aggregates and [Cu₃I₃]-Cyclic Coordination Polymers Supported by Quinolyl-Triazoles. *Dalton Trans.* **2015**, *44*, 6075–6081. [[CrossRef](#)]
36. Cho, S.; Jeon, Y.; Lee, S.; Kim, J.; Kim, T.H. Reversible Transformation between Cubane and Stairstep Cu₄I₄ Clusters Using Heat or Solvent Vapor. *Chem.—A Eur. J.* **2015**, *21*, 1439–1443. [[CrossRef](#)]
37. Vinogradova, K.A.; Shekhovtsov, N.A.; Berezin, A.S.; Sukhikh, T.S.; Rogovoy, M.I.; Artem'ev, A.V.; Bushuev, M.B. Coordination-Induced Emission Enhancement in Copper(I) Iodide Coordination Polymers Supported by 2-(Alkylsulfanyl)Pyrimidines. *Dalton Trans.* **2021**, *50*, 9317–9330. [[CrossRef](#)]
38. Fang, Y.; Soj dak, C.A.; Dey, G.; Teat, S.J.; Li, M.; Cotlet, M.; Zhu, K.; Liu, W.; Wang, L.; O'Carroll, D.M.; et al. Highly Efficient and Very Robust Blue-Excitable Yellow Phosphors Built on Multiple-Stranded One-Dimensional Inorganic–Organic Hybrid Chains. *Chem. Sci.* **2019**, *10*, 5363–5372. [[CrossRef](#)]
39. Vitale, M.; Ryu, C.K.; Palke, W.E.; Ford, P.C. Studies of the Copper(1) Tetramers Cu₄X₄L₄ (X = I, Br, Cl). Effects of Cluster Structure and of Halide on Photophysical Properties. *Inorg. Chem.* **1994**, *33*, 561–566. [[CrossRef](#)]
40. Musina, E.I.; Shamsieva, A.V.; Strelnik, I.D.; Gerasimova, T.P.; Krivolapov, D.B.; Kolesnikov, I.E.; Grachova, E.V.; Tunik, S.P.; Bannwarth, C.; Grimme, S.; et al. Synthesis of Novel Pyridyl Containing Phospholanes and Their Polynuclear Luminescent Copper(I) Complexes. *Dalton Trans.* **2016**, *45*, 2250–2260. [[CrossRef](#)]
41. Yu, Y.D.; Meng, L.B.; Chen, Q.C.; Chen, G.H.; Huang, X.C. Substituent Regulated Photoluminescent Thermochromism in a Rare Type of Octahedral Cu₄I₄ Clusters. *New J. Chem.* **2018**, *42*, 8426–8437. [[CrossRef](#)]
42. Strelnik, I.; Shamsieva, A.; Akhmadgaleev, K.; Gerasimova, T.; Dayanova, I.; Kolesnikov, I.; Fayzullin, R.; Islamov, D.; Musina, E.; Karasik, A.; et al. Emission and Luminescent Vapochromism Control of Octahedral Cu₄I₄ Complexes by Conformationally Restricted P,N Ligands. *Chem.—A Eur. J.* **2023**, *in press*. [[CrossRef](#)]
43. Enikeeva, K.R.; Shamsieva, A.V.; Kasimov, A.I.; Litvinov, I.A.; Lyubina, A.P.; Voloshina, A.D.; Musina, E.I.; Karasik, A.A. Pyridyl-Containing Dialkylphosphine Oxides and Their Chelate Copper(II) Complexes. *Inorg. Chim. Acta.* **2023**, *545*, 121286. [[CrossRef](#)]
44. Price, W.S. Pulsed-field Gradient Nuclear Magnetic Resonance as a Tool for Studying Translational Diffusion: Part 1. Basic Theory. *Concepts Magn. Reson.* **1997**, *9*, 299–336. [[CrossRef](#)]
45. Price, W.S. Pulsed-Field Gradient Nuclear Magnetic Resonance as a Tool for Studying Translational Diffusion: Part II. Experimental Aspects. *Concepts Magn. Reson.* **1998**, *10*, 197–237. [[CrossRef](#)]
46. Kharlamov, S.V.; Latypov, S.K. Modern Diffusion-Ordered NMR Spectroscopy in Chemistry of Supramolecular Systems: The Scope and Limitations. *Russ. Chem. Rev.* **2010**, *79*, 635–653. [[CrossRef](#)]
47. Johnson, C.S. Diffusion Ordered Nuclear Magnetic Resonance Spectroscopy: Principles and Applications. *Prog. Nucl. Magn. Reson. Spec.* **1999**, *34*, 203–256. [[CrossRef](#)]
48. Liu, J.Q.; Luo, Z.D.; Pan, Y.; Kumar Singh, A.; Trivedi, M.; Kumar, A. Recent Developments in Luminescent Coordination Polymers: Designing Strategies, Sensing Application and Theoretical Evidences. *Coord. Chem. Rev.* **2020**, *406*, 213145. [[CrossRef](#)]
49. Dutta, A.; Pan, Y.; Liu, J.Q.; Kumar, A. Multicomponent Isorecticular Metal–Organic Frameworks: Principles, Current Status and Challenges. *Coord. Chem. Rev.* **2021**, *445*, 214074. [[CrossRef](#)]
50. Redmore, D. Phosphorus Derivatives of Nitrogen Heterocycles. 2. Pyridinephosphonic Acid Derivatives. *J. Org. Chem.* **1970**, *35*, 4114–4117. [[CrossRef](#)]
51. Sheldrick, G.M. SHELXT—Integrated Space-Group and Crystal-Structure Determination. *Acta Cryst. A Found Adv.* **2015**, *71*, 3–8. [[CrossRef](#)] [[PubMed](#)]
52. Sheldrick, G.M. Crystal Structure Refinement with SHELXL. *Acta Cryst. C Struct. Chem.* **2015**, *71*, 3–8. [[CrossRef](#)] [[PubMed](#)]
53. Frisch, M.J.; Trucks, G.W.; Schlegel, H.B.; Scuseria, G.E.; Robb, M.A.; Cheeseman, J.R.; Scalmani, G.; Barone, V.; Petersson, G.A.; Nakatsuji, H.; et al. *Gaussian 16, Revision A*; Gaussian, Inc.: Wallingford, CT, USA, 2016.
54. Adamo, C.; Barone, V. Toward Reliable Density Functional Methods without Adjustable Parameters: The PBE0 Model. *J. Chem. Phys.* **1999**, *110*, 6158–6170. [[CrossRef](#)]
55. Weigend, F.; Ahlrichs, R. Balanced Basis Sets of Split Valence, Triple Zeta Valence and Quadruple Zeta Valence Quality for H to Rn: Design and Assessment of Accuracy. *Phys. Chem. Chem. Phys.* **2005**, *7*, 3297. [[CrossRef](#)] [[PubMed](#)]
56. Grimme, S.; Antony, J.; Ehrlich, S.; Krieg, H. A Consistent and Accurate Ab Initio Parametrization of Density Functional Dispersion Correction (DFT-D) for the 94 Elements H–Pu. *J. Chem. Phys.* **2010**, *132*, 154104. [[CrossRef](#)]
57. Johnson, E.R.; Becke, A.D. A Post-Hartree-Fock Model of Intermolecular Interactions: Inclusion of Higher-Order Corrections. *J. Chem. Phys.* **2006**, *124*, 174104. [[CrossRef](#)]
58. Grimme, S.; Ehrlich, S.; Goerigk, L. Effect of the Damping Function in Dispersion Corrected Density Functional Theory. *J. Comput. Chem.* **2011**, *32*, 1456–1465. [[CrossRef](#)]

59. Becke, A.D.; Johnson, E.R. A Density-Functional Model of the Dispersion Interaction. *J. Chem. Phys.* **2005**, *123*, 154101. [[CrossRef](#)]
60. Yanai, T.; Tew, D.; Handy, N. A new hybrid exchange-correlation functional using the Coulomb-attenuating method (CAM-B3LYP). *Chem. Phys. Lett.* **2004**, *393*, 51–57. [[CrossRef](#)]

Disclaimer/Publisher's Note: The statements, opinions and data contained in all publications are solely those of the individual author(s) and contributor(s) and not of MDPI and/or the editor(s). MDPI and/or the editor(s) disclaim responsibility for any injury to people or property resulting from any ideas, methods, instructions or products referred to in the content.